J Appl Electrochem (2011) 41:589–597
DOI 10.1007/s10800-011-0267-2

ORIGINAL PAPER

Screening of PdM and PtM catalysts in a multi-anode direct formic acid fuel cell

Xingwen Yu · Peter G. Pickup

Received: 23 February 2010 / Accepted: 17 February 2011 / Published online: 3 March 2011

Abstract Direct formic acid fuel cells (DFAFC) currently employ either Pt-based or Pd-based anode catalysts for oxidation of formic acid. However, improvements are needed in either the activity of Pt-based catalysts or the stability of Pd-based catalysts. In this study, a number of carbon-supported Pt-based and Pd-based catalysts, were prepared by co-depositing PdM (M = Bi, Mo, or V) on Vulcan® XC-72 carbon black, or depositing another metal (Pb or Sn) on a Pt/C catalyst. These catalysts were systematically evaluated and compared with commercial Pd/C, PtRu/C, and Pt/C catalysts in a multi-anode DFAFC. The PtPb/C and PtSn/C catalysts were found to show significantly higher activities than the commercial Pt/C catalyst, while the PdBi/C provided higher stability than the commercial Pd/C catalyst.

Keywords Direct formic acid fuel cell · Array membrane electrode assemblies · Catalyst screening · Pd, Pt, stability

1 Introduction

With multiple advantages, direct formic acid fuel cell (DFAFC) systems are considered as promising portable power sources [1, 2]. Since the first report of a DFAFC in 1996 [3], both Pt-based and Pd-based catalysts have been widely used at the anode to oxidize formic acid [1, 2, 4–8]. From a fundamental point of view, the electro-oxidation of formic acid on Pt has been recognized as following a so-called "dual pathway" mechanism, as described by Eq. 1 and 2 (CO_{ads} refers to adsorbed carbon monoxide) [9]. Palladium is recognized to be able to facilitate the oxidation of formic acid via the direct dehydrogenation pathway (1) [10], while the indirect pathway (2) is dominant for Pt, which quickly becomes poisoned by the adsorbed CO intermediate. There may also be adsorbed intermediates in the direct pathway, such as formate [11], but these are more weakly adsorbed than CO and have a much smaller inhibitory effect on the oxidation of formic acid. Consequently, Pd can provide much better performances in DFAFC anodes than Pt. However, Pd catalysts deactivate over a period of hours during formic acid oxidation [12], and need to be periodically reactivated. Therefore, improvements of either the activity of Pt-based catalysts or the stability of Pd-based catalysts are two important issues in the development of high performance DFAFCs.

$$\text{Pathway 1: } HCOOH \rightarrow CO_2 + 2H^+ + 2e^- \quad (1)$$

$$\text{Pathway 2: } HCOOH \rightarrow CO_{ads} + H_2O \rightarrow CO_2 + 2H^+ + 2e^- \quad (2)$$

Bimetallic (or trimetallic) catalyst systems are known to have better catalytic activities than pure noble metals for the electro-oxidation of small organic molecules such as methanol, ethanol, and formic acid. A number of Pt alloy, intermetallic, and surface modified catalysts for formic acid oxidation have been introduced in recent years. These include PtRu [13, 14], PtPd [13, 15], PtAu [14, 16, 17], PtBi [18, 19], PtAs [18], PtPb [19–24], and PtSb [23, 25–28], which have all shown better cell performances than pure platinum catalysts. Compared with Pt-based catalysts, the development of Pd-based bimetallic systems for DFAFCs has been relatively sparse. PdAu [29, 30], PdPb [4], PdSn [31, 32], PdSb [7, 33], and PdCo [34] catalysts have shown better performances than Pd.

X. Yu · P. G. Pickup (✉)
Department of Chemistry, Memorial University of Newfoundland, St. John's, NL A1B 3X7, Canada
e-mail: ppickup@mun.ca

Although many bimetallic catalysts have been shown to be superior to pure Pt and/or Pd for formic acid oxidation, there have been few comparisons between different bimetallic catalysts. Such comparisons are extremely important for identifying the best systems for further development, but impossible to make accurately based on published data because of the wide range of catalyst preparation methods and testing conditions that have been employed. In some cases promising results have been demonstrated for bulk electrodes in conventional cells, but the systems have not been evaluated as high surface area catalysts, or in fuel cells.

The purpose of the study reported here was to compare a number of previously reported DFAFC anode catalyst systems in a systematic study. A multi-anode DFAFC has been used to minimize variations in testing conditions and to provide multiple data sets for each catalyst, which allow statistically verifiable comparisons to be made [35]. Catalyst systems were mostly selected based on literature results that were judged to be promising, but not well tested. Thus, PdMo and PdV were selected based on a report by Larsen et al. [36]. PdBi was reported in a patent [37] and has shown better long-term performances than Pd in a DFAFC [38]. PtSn was also reported in a patent [37] and has shown high activity for formic acid oxidation in solution studies [39]. In contrast, PtPb is a relatively well studied system for formic acid oxidation, and has been evaluated in DFAFCs [21, 38, 40]. It was used here in part to provide an assessment of the synthesis and evaluation methods. The very high performances reported here for PtPb validate the methodology employed, and provide a target for new catalysts that are developed.

The synthesis methods employed were guided by the results of previous studies. For the Pd-based systems, co-deposition of Pd with Bi, Mo, or V from aqueous solution by reduction of metal precursors with $NaBH_4$ was selected based of the efficacy of this method for the preparation of carbon-supported PdPb (PdPb/C) catalysts [4]. In contrast, surface modification of a commercial Pt/C catalyst was found to provide very active PtPb/C catalysts [38], and so was also used for the preparation of PtSn/C catalysts.

The compositions of the catalyst evaluated here were selected based on the premise that any metal (M) with beneficial effects on Pt or Pd should exhibit these at low levels, but that these effects might be negated by blocking or dilution of Pt or Pd sites at high levels. Thus, 8:1 Pt:M and Pd:M ratios were initially tested, together with 4:1 ratios in most cases to provide a higher probability of observing an effect. These ratios were also suggested by preliminary studies in which highly active PtPb/C (this study), PdBi/C (this study), PdPb/C [4], and PtSb/C [23] were obtained at these ratios.

2 Experimental

2.1 Preparation of catalysts

2.1.1 PdM/C (M = Mo, V, Bi) bimetallic catalysts

PdM/C (M = Mo, V, Bi) bimetallic catalysts were prepared by a sodium borohydride reduction method [41]. The detailed synthesis procedure was as follows: (1) Pretreatment of carbon black: 200 mg Vulcan® XC-72 carbon black was pretreated by stirring in 10 M HCl (12 h) and then rinsed with deionized water until the pH reached 6–7. (2) The following aqueous solutions were mixed in a 2 L flask: 28 mL of 8 g L^{-1} $PdCl_2$ in 5 M HCl; 2 mL of 5 g L^{-1} polyvinyl alcohol (PVA); 25 mL of 10 g L^{-1} H_3BO_3, and 10 mL of 5 g L^{-1} NH_4F. (3) A certain volume of Mo, V, or Bi precursor solution was added to the flask depending on the targeted mass ratio of Mo, V, or Bi to Pd:

Pd:Mo = 8:1 catalyst: 6.2 mL of 5 g L^{-1} $(NH_4)_6Mo_7O_{24}{\cdot}4H_2O$.
Pd:Mo = 4:1 catalyst: 12.4 mL of 5 g L^{-1} $(NH_4)_6Mo_7O_{24}{\cdot}4H_2O$.
Pd:Bi = 8:1 catalyst: 7.8 mL of 5 g L^{-1} $Bi(NO_3)_3$ in 5 M HNO_3.
Pd:Bi = 4:1 catalyst: 15.6 mL of 5 g L^{-1} $Bi(NO_3)_3$ in 5 M HNO_3.
Pd:V = 8:1 catalyst: 10.5 mL of 5 g L^{-1} VCl_3.
Pd:V = 4:1 catalyst: 21 mL of 5 g L^{-1} VCl_3.

(4) The pretreated Vulcan® XC-72 carbon black (200 mg) and deionized water (1 L) were then added to the flask. (5) The solution was then stirred vigorously while 50 mL of freshly prepared 5 g L^{-1} $NaBH_4$ in deionized water was added drop-wise. (6) The pH of the solution was adjusted to 9–10 by drop-wise addition of 5 M NaOH. (7) The solution was then stirred vigorously for 1 h, after which the catalyst was allowed to settle for 30 min. The carbon-supported Pd-M/C catalyst was then collected by filtration, rinsed with deionized water (five times) and dried at 80 °C for 8 h under vacuum.

2.1.2 PtPb/C and PtSn/C bimetallic catalysts

The Pb modified Pt/C catalyst (PtPb(8:1)/C, the targeted mass ratio of Pt to Pb was 8:1) was prepared by a $NaBH_4$ reduction process as follows: (1) 250 mg of a 20% Pt/C (E-TEK) catalyst was dispersed in 100 mL of DI (de-ionized) water containing 10 drops of 10 M HNO_3 by stirring for 12 h. (2) 2.0 mL of 5 g L^{-1} $Pb(NO_3)_2$ was then added and stirred for 0.5 h. (3) The pH was adjusted to 7 with 20 drops of 5 M NaOH. (4) Dropwise addition of 50 mL of 0.05 M $NaBH_4$ dissolved in DI water, then further stirring for 1 h, and settling for 0.5 h. (5) The product was

collected by filtration and washed well with copious amounts of DI water, then dried at room temperature under vacuum.

Preparation of the Sn modified Pt/C catalysts (PtSn/C) followed a similar procedure, as described previously [42]. XRD analysis [42] showed that the Sn was likely in an amorphous state in the PtSn/C catalysts, and no PtSn alloys could be observed.

2.1.3 Commercial catalysts and formic acid fuel

Commercial catalysts employed for comparison in this study were: (1) 40% Pd/C (40% palladium on Vulcan® XC-72, E-TEK); (2) 20% Pt/C (20% platinum on Vulcan® XC-72, E-TEK); and (3) 20% PtRu/C (20% platinum-ruthenium on Vulcan® XC-72, E-TEK). Formic acid from Alfa Aesar (ACS, 88% + 12% water) was diluted to 5 M with DI water. NMR analysis [43] indicated that before dilution this formic acid contained ca. 3,300 ppm acetic acid (by mass), but no methylformate was detected. Such levels of acetic acid have been shown to decrease the initial current in DFAFCs with Pd anodes [4, 43, 44] and accelerate the rate of deactivation of Pd [4, 44].

2.2 Fuel cell performance tests

2.2.1 Preparation of electrodes

The catalyst was dispersed in a mixture of DI water and a certain volume of Nafion® solution (5%, DuPont) by sonication for 10 min. The mass ratio of net Nafion® to the catalyst was 1:4 in all cases. The resulting ink was deposited onto carbon fiber paper (Toray TGP-H-090) and dried in air for 1 h at room temperature. The loading of the catalyst on the carbon fiber paper was 1.6 mg cm^{-2} (including the carbon support and Nafion®) in all cases. Metal loadings can be calculated from the catalyst compositions reported in Table 1. All electrochemical results are presented based on currents obtained per mg of Pd, Pt, or PtRu (i.e., mass of noble metal).

2.2.2 Multi-anode DFAFC and preparation of anode-array membrane electrode assemblies (MEA)

A multi-anode, liquid-fed fuel cell was used for this study. The details of this cell can be found in [35] and are shown schematically in Fig. 1. This cell is based on a commercial (Electrochem®) 5 cm^2 active area cathode plate, and a custom anode plate with 9 (3 × 3 array) electronically isolated graphite rod anode current collectors embedded in a Lexan plate.

Each anode-array membrane electrode assembly was prepared with a Nafion® 115 membrane (Ion Power), a 5 cm^2 cathode consisting of 4 mg cm^{-2} Pt black on carbon fiber paper, and nine 0.23 cm^2 anodes. The electrodes were hot pressed onto the membrane at 135 °C and 200 kg cm^{-2} for 90 s.

2.2.3 Operation of the cell

The operation of the multi-anode DFAFC was controlled with a multi-channel potentiostat (Arbin®). The cell was operated with 5 M aqueous formic acid fed to the anodes at a flow rate of 0.2 mL min^{-1}, and dry oxygen delivered to the cathode at a flow rate of 100 mL min^{-1} without back pressure. All experiments were conducted at ambient temperature.

It has been established in a previous study [35] that good uniformity and reproducibility are obtained for the operation of each of the 9 anodes. There are no significant effects due to formic acid depletion because of the high concentration used. Since the optimum power density of the DFAFC was usually obtained at cell voltages between 0.5 and 0.3 V [1, 35] these voltages were selected for constant voltage experiments.

Table 1 Crystallite sizes, mass ratios, and metal loadings (wt%) of the catalysts, estimated from XRD, EDX, and TGA analyses

Catalyst (targeted mass ratio)	Crystal size (nm)	Measured mass ratio (mole fraction of M)	Total metal loading (%)	Pd%	Mo%	V%	Bi%	Pt%	Pb%	Sn%
PdMo(4:1)/C	5.3	4.8:1 (0.19)	41.7	34.5	7.2					
PdMo(8:1)/C	5.7	8.9:1 (0.11)	40.0	6.0	4.0					
PdV(4:1)/C	5.6	4.9:1 (0.30)	40.9	34.0		6.9				
PdV(8:1)/C	5.6	9.4:1 (0.18)	39.9	36.1		3.8				
PdBi(4:1)/C	4.2	4.0:1 (0.11)	43.0	34.4			8.6			
PtPb(8:1)/C	2.5	6.2:1 (0.13)	21.8					19.4	2.4	
PtSn(4:1)/C	2.8	3.5:1 (0.32)	24.3					18.9		5.4

Results for the PdBi/C, PtPb/C and PtSn/C catalysts are from previous studies [38, 42]

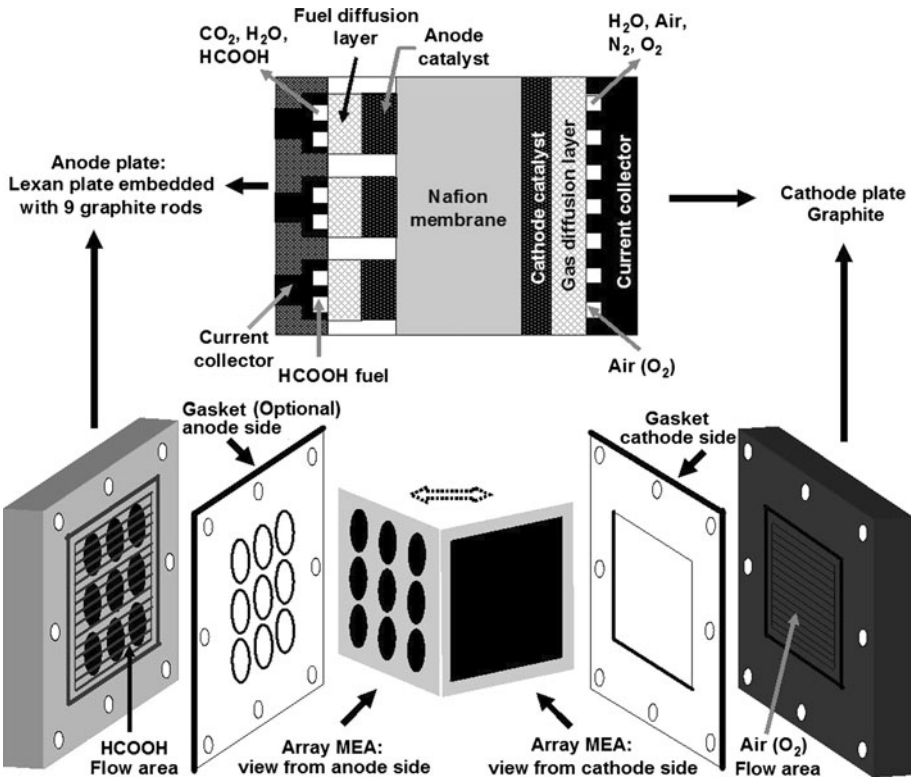

Fig. 1 Schematic diagram of the multi-anode DFAFC

2.3 Characterization of catalysts

2.3.1 Energy dispersive X-ray microanalysis (EDX)

EDX analyses of the catalysts were conducted on a Bruker Xflash 4010 SDD energy dispersive X-ray analyzer.

2.3.2 Thermogravimetric analysis (TGA)

TGA analyses of the catalysts were performed on a TA Instruments Q500 TGA analyzer.

2.3.3 X-ray diffraction (XRD)

XRD patterns of the catalysts were obtained with an X-ray diffractometer (Siemens D500) using a Cu Kα source ($\lambda = 0.15418$ nm) at a scan rate of 0.6° min^{-1}. The scan range was from 30° to 100°.

3 Results

3.1 Characterization of the catalysts

The PdMo/C, PdV/C, PdBi/C, and PtPb/C catalysts were characterized with TGA, EDX, and XRD. Characterization results for the PdBi/C and PtPb/C catalysts have been published elsewhere [38] and are summarized in Table 1.

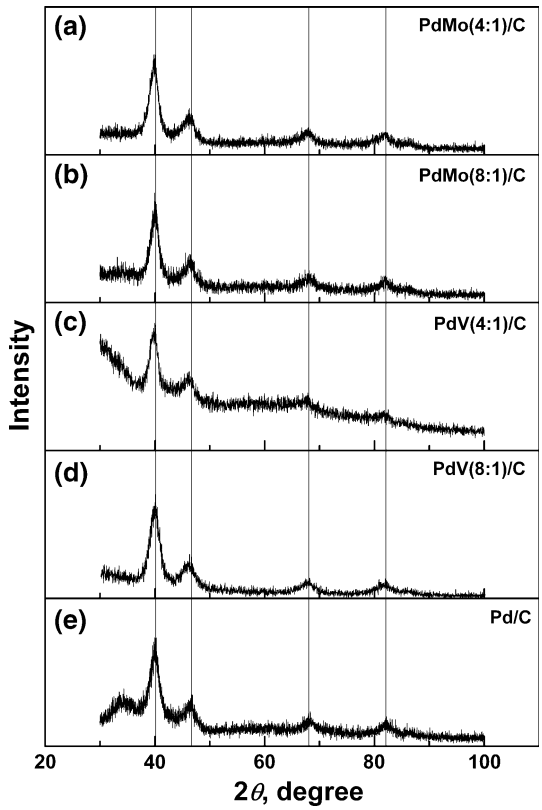

Fig. 2 XRD patterns for the **a** PdMo(4:1)/C; **b** PdMo(8:1)/C; **c** PdV(4:1)/C; **d** PdV(8:1)/C; and **e** Pd/C catalysts

Results for a PtSn/C catalyst, previously analyzed by XPS and XRD [42], are also summarized in Table 1.

Figure 2 shows XRD patterns for the PdMo(4:1)/C, PdMo(8:1)/C, PdV(4:1)/C, PdV(8:1)/C, and Pd/C catalysts. In each pattern, the main peaks for Pd at 40.1°, 46.7°, 68.1°, and 82.1° can be clearly seen. However, no Mo or V peaks can be observed. Relative to Pd/C, there were small shifts of the Pd peaks for the PdMo(4:1)/C and PdV(4:1)/C catalysts, which suggests that the Mo and V were alloyed with the Pd. These results are consistent with previous studies of the PdPb/C and PdBi/C catalysts in which the Pd peaks were shifted by the presence of Pb or Bi [4, 38]. Crystallite sizes for the PdMo/C and PdV/C catalysts estimated from the XRD patterns according to the Scherrer equation are summarized in Table 1.

The Pd:Mo and Pd:V mass ratios in the catalysts were analyzed by EDX, as summarized in Table 1. The metal loadings of the catalysts were analyzed by TGA. For these analyses, the residual mass upon heating of the PdMo/C or PdV/C catalysts to 750 °C was attributed to Pd and MoO_3 or V_2O_5. Pd, Mo, and V loadings for the PdMo/C and PdV/C catalysts, estimated from the EDX and TGA results, are summarized in Table 1.

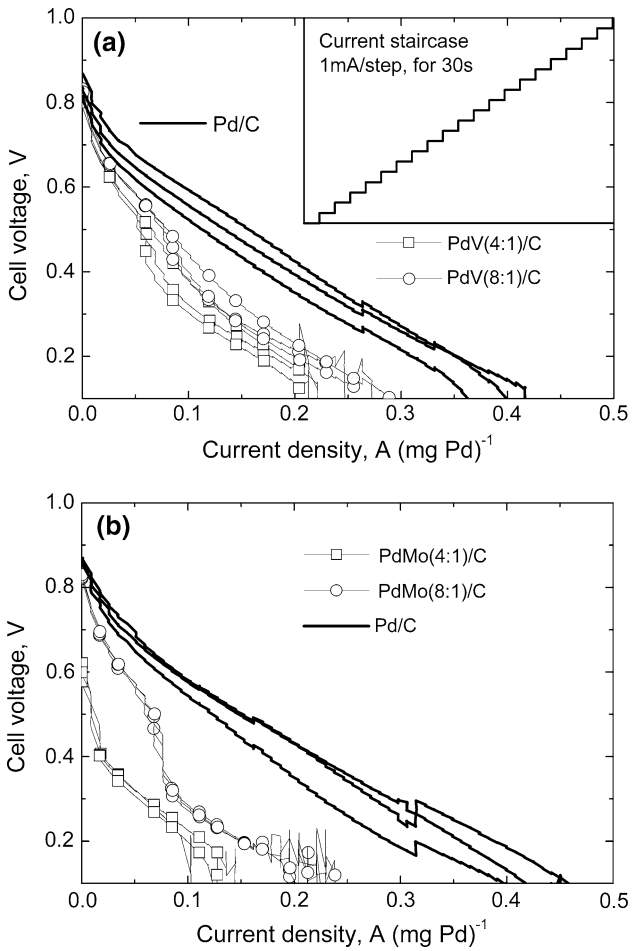

Fig. 3 Polarization plots for Pd/C (**a**, **b**), PdV/C (**a**) and PdMo/C (**b**) catalysts in multi-anode DFAFCs. Currents have been normalized on the basis of the Pd mass. Data for three different electrodes of each type in the same MEA are shown

3.2 Comparison of PdMo/C and PdV/C with commercial Pd/C

The PdMo/C and PdV/C catalysts were studied by comparison with a commercial Pd/C catalyst in the multi-anode DFAFC. Anode-array MEAs were prepared with either three electrodes each of PdMo(4:1)/C, PdMo(8:1)/C, and Pd/C, or three electrodes each of PdV(4:1)/C, PdV(8:1)/C, and Pd/C. A current staircase polarization mode was employed to obtain polarization curves, as illustrated in the inset of Fig. 3a. In this mode, the current applied to each of the anodes was stepped in 1 mA intervals from zero, with 30 s at each current for the potential to stabilize.

Figure 3a and b show groups of polarization curves obtained with the PdV/C, PdMo/C, and Pd/C anode catalysts. The currents in these polarization plots have been normalized based on the mass of Pd. The reproducibility of the polarization measurements for each type of catalyst was acceptable (the voltage jumps at about 0.3 V in these figures are most likely due to spikes in the mains voltage). The commercial Pd/C catalyst provided excellent performance, generating a maximum normalized power of ca. 90 mW $(\text{mg Pd})^{-1}$, while both the PdMo/C and PdV/C catalysts provided poor cell performances. The differences can be seen to be statistically significant relative to the differences between electrodes of the same type. It is also seen that increasing the proportion of Mo or V in the catalyst lowered the performance further relative to pure Pd.

The characterization results for the PdMo/C and PdV/C catalysts shown in Fig. 2 and Table 1 do not reveal any significant differences in terms of crystallite sizes, alloying characteristics and Pd loading from the much more active PdPb/C and PdBi/C catalysts that have been reported [4, 38]. This provides strong evidence that both Mo and V poison Pd through some electronic and/or chemical effect. It therefore appears unlikely that useful PdMo or PdV alloy catalysts can be developed for formic acid oxidation.

3.3 Comparison of PdBi/C with commercial Pd/C

The performance of a PdBi(4:1)/C catalyst prepared by co-deposition of Pd and Bi on Vulcan® XC-72 was compared with that of commercial Pd/C in the multi-anode fuel cell following a procedure similar to that used for PdMo/C and PdV/C. In order to obtain a more statistically significant comparison, the MEA was prepared with five PdBi(4:1)/C electrodes and four Pd/C electrodes. Polarization curves were obtained in a potential staircase mode,

in which the anodes were simultaneously polarized from the cells' open circuit voltage (OCV) of 0.9 V to a final voltage of 0.3 V, with voltage steps of −15 mV. The current at each step was allowed to stabilize for 30 s.

Figure 4 shows consecutive polarization curves in which the anodes were continuously polarized between 0.9 and 0.3 V for 12 cycles. The cell voltage was returned to the original OCV at the end of each polarization (causing increasingly negative currents at the beginning of the polarization curves as the catalysts deactivated), and the next polarization was begun immediately. The currents in these polarization plots have again been normalized on the basis of the Pd mass. As seen in the figure, the performances of the PdBi(4:1)/C electrodes were lower than for the Pd/C electrodes during the first few polarizations. The performances of both sets of electrodes decreased during repeated polarizations due to deactivation of the anode catalysts. However, the deactivation rate of the PdBi/C catalyst was evidently slower than for the Pd/C catalyst, such that after 6 or 7 cycles, the performances of the PdBi/C electrodes exceeded those of the Pd/C electrodes.

Figure 5 further compares the stabilities of the PdBi/C and Pd/C catalysts by showing the current decay during operation of the cell at a fixed voltage of 0.3 V. Although the initial currents at the PdBi/C electrodes were lower than for the Pd/C electrodes, the current decay at PdBi/C was significantly slower. The currents at the PdBi/C electrodes exceed those at the Pd/C electrodes after ca. 1 h of continuous operation, and the advantage of the PdBi/C catalyst became more evident with increasing operating time.

3.4 Comparison of PtPb/C with commercial Pt/C and PtRu/C catalysts

An anode-array MEA was prepared with three electrodes each of PtPb(8:1)/C, PtRu/C, and Pt/C. Figure 6 shows a series of consecutive polarization curves in which the cell voltage was returned to the initial OCV at the end of each polarization, and the next polarization was begun immediately. The OCV for the PtPb(8:1)/C anodes (ca. 0.85 V) was ca. 150 mV higher than for the PtRu/C (ca. 0.7 V) and Pt/C (ca. 0.7 V) anodes. The normalized currents for the PtPb(8:1)/C anodes were significantly higher than for the PtRu/C and Pt/C anodes at all cell voltages (from 0.75 to 0.1 V).

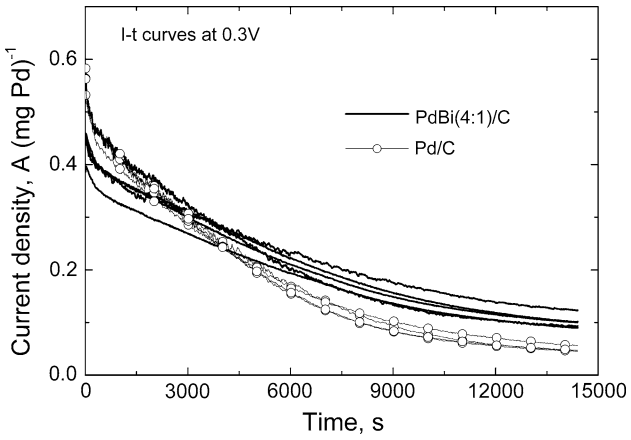

Fig. 5 Current versus time curves at a cell voltage of 0.3 V for PdBi(4:1)/C anodes (data for five different electrodes in the same MEA are shown) and Pd/C anodes (four electrodes in the MEA) in a multi-anode DFAFC. Currents have been normalized on the basis of the Pd mass

Figure 7 shows specific current versus time plots for the PtPb(8:1)/C, PtRu/C and Pt/C anodes during operation at a constant cell voltage of 0.5 V. The specific currents for the PtPb(8:1)/C electrodes were much higher than for either the PtRu/C or Pt/C electrodes. All three catalysts exhibited some decay in performance with time, following an initial increase in performance in most cases. However, the performance losses were much less than for Pd-based catalysts (Fig. 5). Notably, the PtPb(8:1)/C catalyst exhibited good performance stability at 0.5 V, with the average current at 2 h being higher than during the first 1.5 min. Even though a higher cell voltage was used here (to emphasize the performance of the PtPb), currents at the PtPb(8:1)/C electrodes were higher than those obtained with Pd/C and

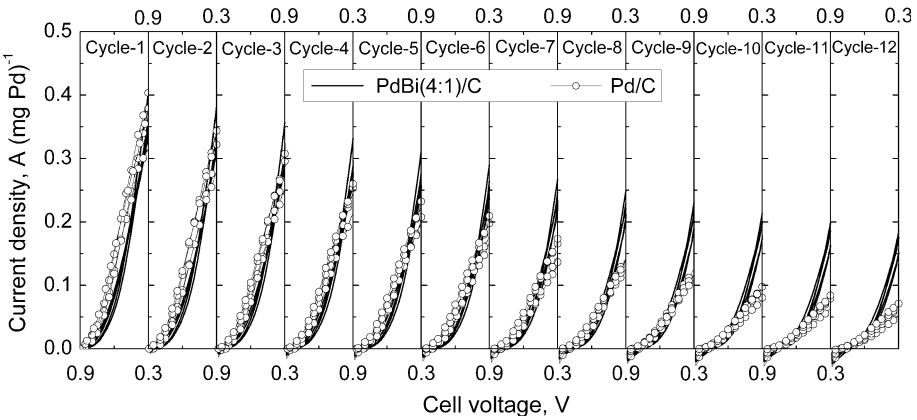

Fig. 4 Consecutive polarization curves (voltage staircase) for PdBi(4:1)/C anodes (data for five different electrodes in the same MEA are shown) and Pd/C anodes (four electrodes in the MEA) in a multi-anode DFAFC. Currents have been normalized on the basis of the Pd mass

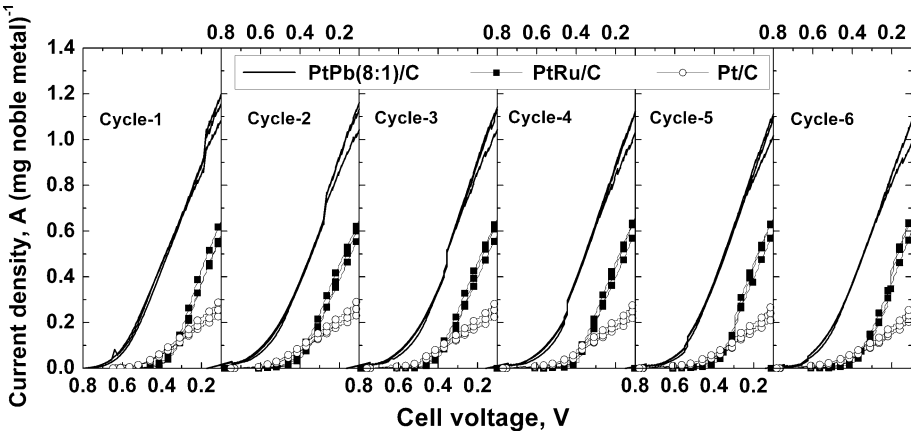

Fig. 6 Consecutive polarization curves (voltage staircase) for PtPb(8:1)/C, Pt/C and PtRu/C anodes (three electrodes of each in the same MEA) in a multi-anode DFAFC. Currents have been normalized on the basis of the Pt or PtRu mass

PdBi/C electrodes at 0.3 V for times over ca. 4,000 s. A comparison of results at 0.3 V is made in Sect. 4.

3.5 Comparison of PtSn/C and Pt/C catalysts

PtSn(8:1)/C and PtSn(4:1)/C catalysts, prepared by modification of 20% Pt/C, were compared with the commercial Pt/C catalyst in the multi-anode DFAFC. An anode-array MEA was prepared with three electrodes each of PtSn(4:1)/C, PtSn(8:1)/C, and Pt/C.

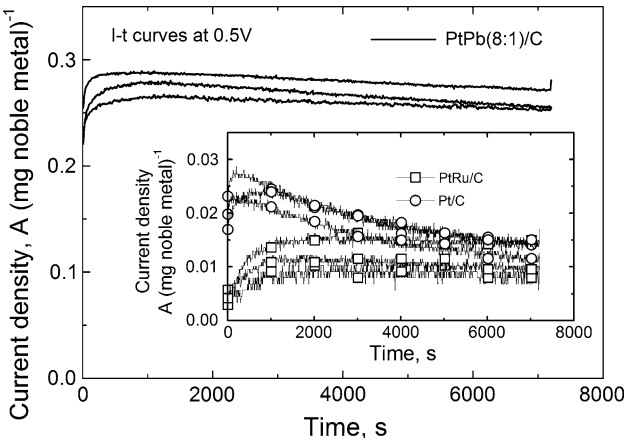

Fig. 7 Current versus time curves for PtPb(8:1)/C, Pt/C and PtRu/C anodes (three electrodes of each in the same MEA) in a multi-anode DFAFC, at cell operation voltages of 0.5 V. Currents have been normalized on the basis of the Pt or PtRu mass

Figure 8 shows a series of consecutive polarization curves for this MEA. The currents shown in this figure were normalized on the basis of the Pt mass. As seen in Fig. 8, the PtSn(8:1)/C catalyst showed the highest activity among the three catalysts, while the PtSn(4:1)/C catalyst was only slightly superior to Pt/C.

Specific current versus time plots for the PtSn(4:1)/C, PtSn(8:1)/C, and Pt/C electrodes during operation at a constant cell voltages of 0.3 V are shown in Fig. 9. Consistent with the results of Fig. 8, the specific currents for the PtSn/C catalysts were higher than for Pt/C. Both the PtSn/C and Pt/C catalysts exhibited some decay in performance with time, following an initial increase in performance.

4 Discussion

The purpose of the study described here was to compare the performances of various types of catalyst under a uniform set of conditions. This was the beginning of a systematic study aimed at identifying the most suitable

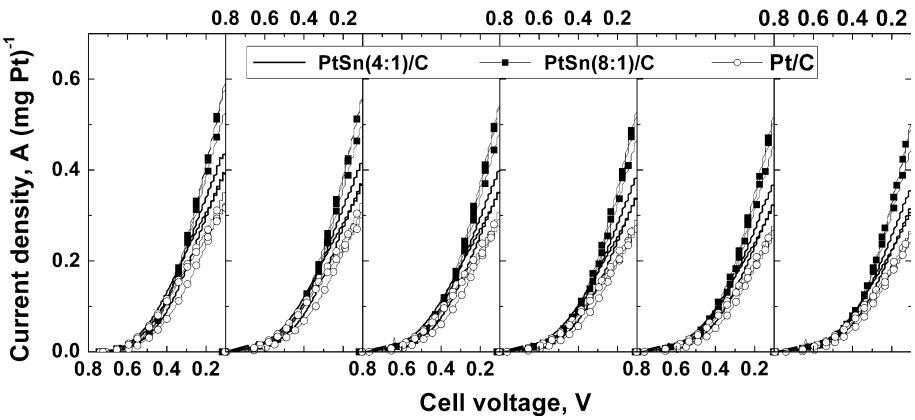

Fig. 8 Consecutive polarization curves (voltage staircase) for PtSn(4:1)/C, PtSn(8:1)/C and Pt/C anodes (three electrodes of each in the same MEA) in a multi-anode DFAFC. Currents have been normalized on the basis of the Pt mass

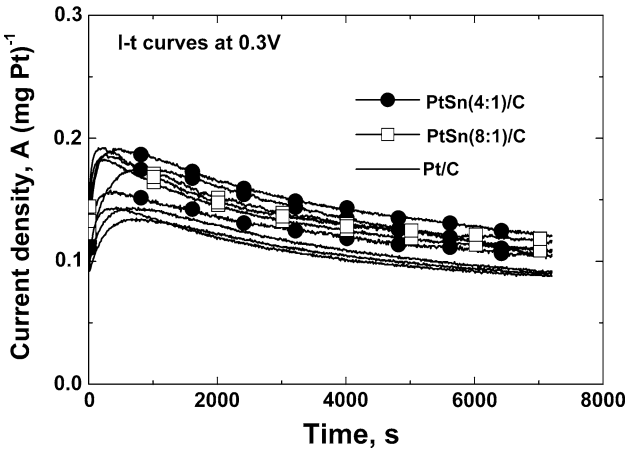

Fig. 9 Current versus time curves for PtSn(4:1)/C, PtSn(8:1)/C and Pt/C (three electrodes of each in the same MEA) in a multi-anode DFAFC, at cell operation voltages of 0.3 V. Currents have been normalized on the basis of the Pt mass

catalyst systems for development as DFAFC anodes. While not comprehensive, nor definitive, the results do provide useful guidance regarding which metals and synthesis methods offer the best prospects. As such, the negative results reported here for PdMo and PdV are important in light of the positive results for PdBi under the same conditions and with the same synthesis method. They indicate that it is unlikely that useful PdMo and PdV alloy catalysts can be developed for DFAFCs. Likewise, the results for PtSn, while showing an improvement over Pt, are put into context by the far superior results for PtPb.

Results for operation of the catalysts at a constant cell voltage of 0.3 V are summarized in Fig. 10. This figure clearly shows that PtPb was significantly better than all of the other catalysts at all timescales studied (up to 4 h). It also shows the superiority of Pd over Pt at short times

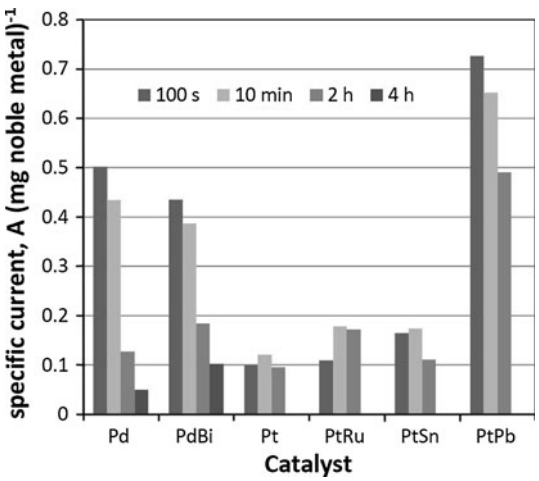

Fig. 10 Average specific currents at 100 s, 10 min, 2 h, and 4 h for DFAFCs at 0.3 V with the specified anode catalysts

(100 s), and the reversal in this superiority at long times (4 h). PdBi is attractive relative to Pd because of its slower deactivation, but was inferior to the PtPb at long times. Results for PdMo/C and PdV/C and are not included in Fig. 10 because these catalysts performed so poorly relative to Pd/C. We suggest that a previous report [36] of apparent high activities for formic acid oxidation with these combinations of metals may have been due to electrochemical corrosion of the Mo and V supports that were used.

The performances of the surface modified PtSn/C catalysts reported here are low relative to those reported for PtSn alloys [37, 39]. This is surprising since the same surface modified catalysts have been shown to provide excellent performances in direct ethanol fuel cells [42], and the similarly prepared PtPb/C catalysts are outstanding in the DFAFC. The disappointing performances of the surface-modified PtSn/C catalysts may have been due to the deposition of the Sn as an oxide [42] (or its oxidation by air following deposition), since it has been shown that electrodes prepared by mixing SnO_2 and Pt are less active in a DFAFC than PtSn alloys [37]. Nevertheless, the results here do confirm that Sn has a beneficial effect on formic acid oxidation at Pt, even if only present as an oxide layer on the Pt surface. The much lower effect relative to that of Pb (Fig. 7) which has also been found to be present as a surface oxide [23], suggests a fundamentally different mode of action, although it is possible that one, or both, of these oxides become reduced to zero valent metal atoms in the DFAFC.

Since PtPb is clearly the most promising system for further development, the remainder of this section presents a brief comparison with the two other reports of the use of PtPb based catalysts in DFAFCs. Uhm et al. [21] reported the use of a catalyst prepared by electrochemical underpotential deposition of a monolayer of Pb onto a commercial Pt/C catalyst. The current produced by their DFAFC at 0.3 V and 60 °C was increased by ca. 40% by the presence of the Pb, but this advantage was lost after 5 polarization cycles. However, much better and more stable performances were obtained when a layer of unmodified catalyst was coated onto the modified catalyst layer to inhibit loss of Pb. Liu et al. [40] have reported similar performances with a chemically prepared PtPb intermetallic catalyst, but used a much higher anode catalyst loading (3.2 vs. 1 mg cm^{-2} metal loading) and a temperature of 70 °C.

On a Pt mass basis, the performances shown in Figs. 6 and 7 for the chemically prepared PtPb(8:1)/C studied here significantly exceed those reported in ref. [21], despite the use of a lower cell operating temperature (30 vs. 60 °C). Furthermore, the stability seen in Fig. 7 is comparable to that reported in ref. [21] for the bilayer electrode. Although

PtPb intermetallic catalysts may exhibit better long-term durability [22], the limited DFAFC cell data available at the moment suggests that they may have lower specific activities than surface modified PtPb catalysts.

5 Conclusions

The use of a multi-anode fuel cell provides an efficient method for the screening of DFAFC anode catalysts and assessing the statistical significance of differences between catalysts. This study has revealed that surface modification of a Pt/C catalyst with Pb by chemical reduction with $NaBH_4$ can produce catalysts with high performances. However, similarly prepared PtSn/C catalysts are inferior to both the PtPb/C catalyst and PtSn alloys. Pt-based catalysts are shown to be superior to Pd-based catalyst after 4 h of operation due to rapid decay of the activities of the Pd-based materials. Although a PdBi/C alloy catalyst exhibited better stability than Pd itself, its performance over all timescales (to 4 h) was greatly inferior to that of the best Pt-based catalyst (PtPb).

Acknowledgments This study was supported by the Natural Sciences and Engineering Research Council of Canada (NSERC) through a Strategic Projects Grant in partnership with Tekion (Canada) Inc., and by Memorial University.

References

1. Yu X, Pickup PG (2008) J Power Sources 177:124
2. Uhm S, Lee HJ et al (2009) Phys Chem Chem Phys 11:9326
3. Weber M, Wang JT et al (1996) J Electrochem Soc 143:L158
4. Yu X, Pickup PG (2009) J Power Sources 192:279
5. Wu YN, Liao SJ et al (2010) J Power Sources 195:6459
6. Kang YY, Ren MJ et al (2010) Electrochim Acta 55:5274
7. Haan JL, Stafford KM et al (2010) Electrochim Acta 55:2477
8. Haan JL, Stafford KM et al (2010) J Phys Chem C 114:11665
9. Feliu JM, Herrero E et al (2003) In: Vielstich W, Gasteiger HA (eds) Handbook of Fuel Cells, vol 2. Wiley, New York, p 679
10. Garin F (2004) Catal Today 89:255
11. Samjeske G, Miki A et al (2006) J Phys Chem B 110:16559
12. Pan Y, Zhang R et al (2009) Electrochem Solid State Lett 12:B23
13. Rice C, Ha S et al (2003) J Power Sources 115:229
14. Choi JH, Jeong KJ et al (2006) J Power Sources 163:71
15. Waszczuk P, Barnard TM et al (2002) Electrochem Commun 4:599
16. Zhang S, Shao YY et al (2010) J Power Sources 195:1103
17. Bai YC, Zhang WD et al (2011) J Alloys Compd 509:1029
18. Herrero E, Fernandez-Vega A et al (1993) J Electroanal Chem 350:73
19. Volpe D, Casado-Rivera E et al (2004) J Electrochem Soc 151:A971
20. Zhang LJ, Wang ZY et al (2006) J Alloys Compd 426:268
21. Uhm SY, Chung ST et al (2007) Electrochem Commun 9:2027
22. Matsumoto F, Roychowdhury C et al (2008) J Electrochem Soc 155:B148
23. Yu X, Pickup PG (2010) Electrochim Acta 55:7354
24. Ji XL, Lee KT et al (2010) Nat Chem 2:286
25. Casado-Rivera E, Volpe DJ et al (2004) J Am Chem Soc 126:4043
26. Lee JK, Jeon H et al (2008) Electrochim Acta 53:6089
27. Peng B, Wang JY et al (2009) Electrochem Commun 11:831
28. Peng B, Wang HF et al (2010) J Phys Chem C 114:3102
29. Larsen R, Ha S et al (2006) J Power Sources 157:78
30. Jiang JH, Kucernak A (2009) Electrochim Acta 54:4545
31. Zhang ZH, Ge JJ et al (2009) Fuel Cells 9:114
32. Liu ZL, Zhang XH (2009) Electrochem Commun 11:1667
33. Yu XW, Pickup PG (2010) Electrochem Commun 12:800
34. Morales-Acosta D, Ledesma-Garcia J et al (2010) J Power Sources 195:461
35. Yu X, Pickup PG (2009) J Power Sources 187:493
36. Larsen R, Zakzeski J et al (2005) Electrochem Solid State Lett 8:A291
37. Iordache C, Blair S, et al (2008) World Patent : WO 2008/080227 Al
38. Yu X, Pickup PG (2009) Int J Green Energy 6:571
39. Yi QF, Zhang JJ et al (2008) J Appl Electrochem 38:695
40. Liu ZL, Guo B et al (2008) J Power Sources 184:16
41. Zhang LL, Lu TH et al (2006) Electrochem Commun 8:1625
42. Li G, Pickup PG (2007) J Power Sources 173:121
43. Law WL, Platt AM et al (2009) J Electrochem Soc 156:B553
44. Masel RI, Zhu Y, et al (2007) UK Patent: GB2424650B